Available online at www.sciencedirect.com
SCIENCE DIRECT®
Polymer 45 (2004) 3487–3496
polymer
www.elsevier.com/locate/polymer

Rheological behavior of new melt compounded copolyamide nanocomposites

L. Incarnato[a,*], P. Scarfato[a], L. Scatteia[b], D. Acierno[c]

[a]Department of Chemical and Food Engineering, University of Salerno, Via Ponte don Melillo, 84084 Fisciano (SA), Italy
[b]TEMA (Advanced Materials and Manufacturing Technologies) Italian Aerospace Research Center, Via Maiorise, 81043 Capua (CE), Italy
[c]Department of Materials and Production Engineering, University of Naples 'Federico II', P.le Tecchio 80, 80125 Napoli, Italy

Received 12 December 2003; received in revised form 1 March 2004; accepted 4 March 2004

Abstract

In this paper the rheological behavior of new polyamide-based nanocomposites produced by melt compounding using three different silicate loadings and screw speeds was investigated. The thermoplastic matrices selected were a polyamide 6 and its statistical copolymer having partially aromatic structure, whereas the clay was a commercial organo-modified montmorillonite. Hybrid systems were prepared by means of a laboratory-scale twin screw extruder and were submitted to rheological and structural investigations. The rheological experiments (dynamic frequency sweep, steady rate sweep and stress relaxation tests) were performed to evaluate the effect of both system composition (kind of matrix and clay content) and extrusion rate on the flow behavior of the nanocomposites. Rheology, that is highly sensitive to the nanoscale structure of the materials, put out a pseudo-solid like flow behavior at long times in the hybrids with silicate content higher than 6 wt% and produced with high extrusion rate; this response was related to the formation of an extended structural network across the polymer matrix due to strong polymer–silicate interactions that slow the relaxation times of the macromolecules. Corresponding to this behavior, TEM micrographs have shown a quite uniform dispersion of clay particles on micron-scale and a fair level of silicate exfoliation on nanoscale with a macroscopic preferential orientation of the layers in samples. The rheological measurements also reveal that this flow response is more marked for nanocomposites based on the copolyamide matrix, suggesting that this resin may have a higher silicate affinity respect to polyamide 6 homopolymer.

Keywords: Copolyamide nanocomposites; Melt compounding; Rheology

1. Introduction

Among engineered thermoplastic polymers, polyamides have a wide and continuously growing market spread, due to their favorable properties (chemical and mechanical resistance, low permeability respect to gases and vapors, high optical transparency, printability, etc.) [1–3]. In particular, the most common applicative fields for polyamide resins are packaging, automotive, textile, etc. Recent noteworthy scientific researches have demonstrated that numerous properties of interest for these industrial productions can be at the same time improved, maintaining a profitable performance/cost ratio, by reinforcement of polyamides using nanoscale layered clay minerals as fillers [4–11]. In particular, a great attention is devoting towards polyamide-based nanocomposites prepared by melt compounding: this processing approach, in fact, seems to be very promising from an industrial and a commercial point of view since the resulting materials not only exhibit performance improvement but also maintain good compatibility with the conventional polymer processing techniques, so they can be easily extruded or molded to near-final shape [4,12–18]. The technological relevance of these nanocomposite systems is testified by the numerous patents issued over the last few years [18–25], also if to date only few products have entered the market. At present time, one of the main limit to commercialization of melt compounded polyamide-based nanocomposites arises from the difficulty in controlling the morphology (clay dispersion and exfoliation degree, matrix crystallinity, clay and polymer orientation) developed during the production process, that in turn affects the ultimate material limits [4,10,14–18]. Moreover, due to reduced thermal stability

* Corresponding author. Tel.: +39-089964144; fax: +39-089964057.
E-mail address: lincarnato@unisa.it (L. Incarnato).

0032-3861/$ - see front matter © 2004 Elsevier Ltd. All rights reserved.
doi:10.1016/j.polymer.2004.03.005

of the organoclay, the processing temperatures and the organoclay used have to be opportunely selected to guarantee the maximum performance of melt compounded nanocomposites [4,16,26]. Although significant progress has been made in analyzing the manifold relationships between system composition, processing parameters, morphology and end properties of polyamide–silicate nanocomposites, a general understanding has yet to emerge and some more theoretical and experimental studies are indispensable.

In this field, we are performing a research project having the aim to obtain melt compounded polyamide–silicate nanocomposites with improved processability and properties. At this regard, we have analyzed a new melt compounded nanocomposite system based on a copolymer of polyamide 6 as matrix. The selected copolyamide was a commercial resin (traded by Caffaro SpA, Italy, as ADS 40T) containing random the comonomer 1,1′,3-trimethylcyclohexil-3-methylamine-5-isophtalamide at 5 wt%. As known, the inclusion of a comonomer in a polymer chain assures a depression of the melting point of the resin [27], what can allow the extrusion temperature lowering with respect to the homopolymer case. Moreover, the rigid, partially aromatic nature of the comonomer used in this study could also stabilize extended conformational arrangements of the macromolecules making easier their intercalation in the organoclay galleries, so increasing the polymer–silicate affinity. From these considerations, and on the basis of other our experimental results on copolyamide-based packaging films [28], ADS 40T copolymer appears a promising material to reach our objectives. The first results of the research were reported and discussed in detail in a previous paper [29] on preparation and characterization of these new melt compounded nanocomposites based on the ADS copolyamide. In particular, in order to understand the processing-morphology-property relationships, the effects of different silicate loadings and extrusion speeds on clay dispersion, exfoliation level and thermal response of the hybrids were evaluated. Afterwards, this second part of the research was focused on the rheological characterization of the same copolyamide-based nanocomposite systems, since viscoelastic measurements are highly sensitive to the nanoscale structure of the hybrids and appear to be a powerful method to probe the developed structure of such materials. Moreover, to highlight the effect of comonomer on the polymer–clay affinity and then on the morphology of the hybrids, the rheological behavior of the samples was also compared with that shown by nanocomposites produced at the same processing conditions using a polyamide 6 homopolymer as a matrix.

2. Experimental

2.1. Materials

The silicate used for nanocomposite preparation was the Cloisite 30B (supplied by Southern Clay Products, Inc.), a layered sodium montmorillonite organically modified by methyl, tallow, bis-2-hydroxyethyl, quaternary ammonium chloride (90 meq/100 g clay), having interlayer basal spacing $d_{001} = 18.5$ Å. The two polyamide matrices, both supplied by Caffaro SpA (Italy), were a nylon 6 standard (PA6 F34L, IV = 3.4 dl/g) and its statistical copolymer (ADS 40T, IV = 2.9 dl/g) containing the comonomer 1,1′,3-trimethylcicloesil-3,metilamine-5,isoftalamide at 5 wt%. The molecular structure of ADS copolyamide is shown in Fig. 1.

2.2. Melt processing

The polyamide-layered silicate nanocomposites were prepared by melt compounding using an Haake twin-screw extruder having counter-rotating intermeshing cone-shaped screws with $L = 300$ mm. The adopted screw design allows to have varying degrees of mixing along the length of the screws. A temperature profile of 265–260–255–245 °C from hopper to die, respectively, was imposed and a circular die having $D = 1$ mm was used.

Prior to the processing, the materials were dried in a vacuum oven at 87 °C for 18 h obtaining a moisture level below 0.2 wt% in order to avoid bubble formation and polymer degradation during processing [20]. Nanocomposite tapes at different organoclay content (3, 6 and 9 wt%) were extruded at three screw speeds: 50, 80 and 100 rpm, corresponding to average residence times in the extruder of about 3.5, 3.0 and 2.5 min, respectively. The processing conditions and the sample nomenclature used for the discussion of results are reported in Table 1.

2.3. Characterization

Calorimetric measurements on neat ADS and PA6 matrices were performed with a Mettler differential scanning calorimeter mod. DSC30. The samples were first heated from 0 to 260 °C and held at this temperature for 10 min to remove their thermo-mechanical history; then, they were cooled to 0 °C and re-heated to 260 °C. A scan rate of 10 °C/min was used for all the runs. The values of melting temperature T_m and enthalpy ΔH_m were obtained from the second heating scan.

Transmission electron microscopy (TEM) analysis was conducted using a Philips EM 208 with different magnification levels. The images were captured on sections located normal to the extrusion direction, prepared by microtoming

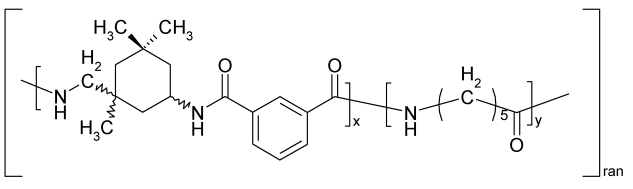

Fig. 1. Molecular structure of ADS copolyamide.

Table 1
Processing conditions and sample nomenclature

Nominal wt% of Cloisite 30B	Screw speed (rpm)	ADS40T-based hybrids	PA6-based hybrids
3	50	3ADS-50	3PA6-50
	80	3ADS-80	3PA6-80
	100	3ADS-100	3PA6-100
6	50	6ADS-50	6PA6-50
	80	6ADS-80	6PA6-80
	100	6ADS-100	6PA6-100
9	50	9ADS-50	9PA6-50
	80	9ADS-80	9PA6-80
	100	9ADS-100	9PA6-100

of ultra-thin specimens with a Leica Utracut UCT microtome.

Rheological measurements were performed using an ARES rotational rheometer (Rheometrics, Inc.) with a parallel plates geometry (plate diameter = 25 mm, gap of 0.5 mm). All samples were tested at 255 °C after drying at 87 °C in a vacuum oven for 18 h, in order to prevent moisture induced degradation phenomena. Dynamic frequency sweep tests were executed in the frequency range of 0.1–100 rad/s using a strain amplitude of 1%, proven to be in the linear viscoelasticity range by means of strain sweep measurements. Transient stress relaxation measurements in linear regime were taken with a single-step strain $\gamma_0 = 1\%$ applied at $t = 0$, measuring the shear stress $\sigma(t)$ as a function of time and obtaining the linear stress relaxation modulus $G(t)$ as $G(t) = \sigma(t)/\gamma_0$. Steady rate sweep test were performed in the shear rate range of $0.1–90\ s^{-1}$. All experiments were carried out under a nitrogen atmosphere to avoid thermo-oxidative degradation phenomena of the specimens.

Dynamic-mechanical analysis was carried out using a TA Instruments DMA 2980 analyzer. DMA spectra were recorded in the tensile mode, with an oscillation amplitude of 1 μm, a frequency of 1 Hz and a heating rate of 5 °C/min in the range of −50–250 °C.

3. Results and discussion

A main need in producing polymer–silicate nanocomposites by melt compounding process is to opportunely select the polymer–organoclay system so to avoid their thermal degradation and to optimize their chemical affinity. In this framework the ADS commercial resin, a copolymer of nylon 6 containing random the comonomer 1,1′,3-trimethylcyclohexil-3-methylamine-5-isophtalamide at 5 wt%, was investigated as an alternative polyamide matrix. It is known, in fact, that comonomers can affect both intermolecular and intramolecular interactions inducing significant changes in the crystallization process of a polyamide [2,3,28,30]. Incorporating a comonomer into PA6 homopolymer chain, a depression of the melting point was assured, what can allow to use lower extrusion temperatures with respect to the homopolymer; this feature has a main role in melt compounding due to restricted thermal stability of organoclays. DSC measurements performed on neat ADS and PA6 have evidenced that ADS matrix exhibits lower melting temperature and enthalpy with respect to PA6, as expected. In particular, the T_m value measured for ADS sample is about 5 °C lower than for the homopolymer, as can be clearly seen in the second heating scan of the DSC thermograms corresponding to both matrices, compared in Fig. 2. Moreover, due to the rigid, partially aromatic nature of the comonomer contained in the ADS resin, extended conformational arrangements of the macromolecules could be stabilized making easier the polymer intercalation in the organoclay galleries. At this regard, in an our previous work on preparation and structural characterization of melt compounded ADS-based nanocomposites it was verified that strong polymer–silicate interactions are present in such systems [29]. Since the meso and nanoscale structure of polymer systems [4,31–34] highly affects their viscoelastic response, in this second part of the research we have investigated the relationships between composition, processing conditions, morphology and rheology of melt compounded polyamide nanocomposites. With this aim, ADS-based hybrid systems

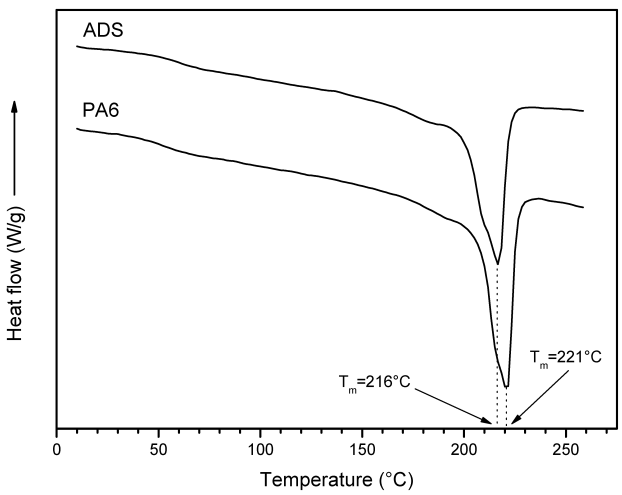

Fig. 2. Comparison between the second heating run of DSC thermograms obtained for the ADS and PA6 matrices.

were produced using three different organoclay amounts and extrusion rates and their rheological behavior was analysed and related to sample morphology. The same study was also performed on PA6-based hybrid systems, for comparison purpose.

In Fig. 3(a) and (b) the complex viscosity curves of ADS-based nanocomposites at different clay content and extrusion rates are compared. While the matrix displays a pseudo-Newtonian behavior in almost the whole range of angular frequency, nanocomposite samples show an higher complex viscosity and a more pronounced shear thinning behavior with the increase of silicate loading, at fixed extrusion rate (Fig. 3(a)). Shear thinning pseudo-non-Newtonian behavior is observed in some conventional

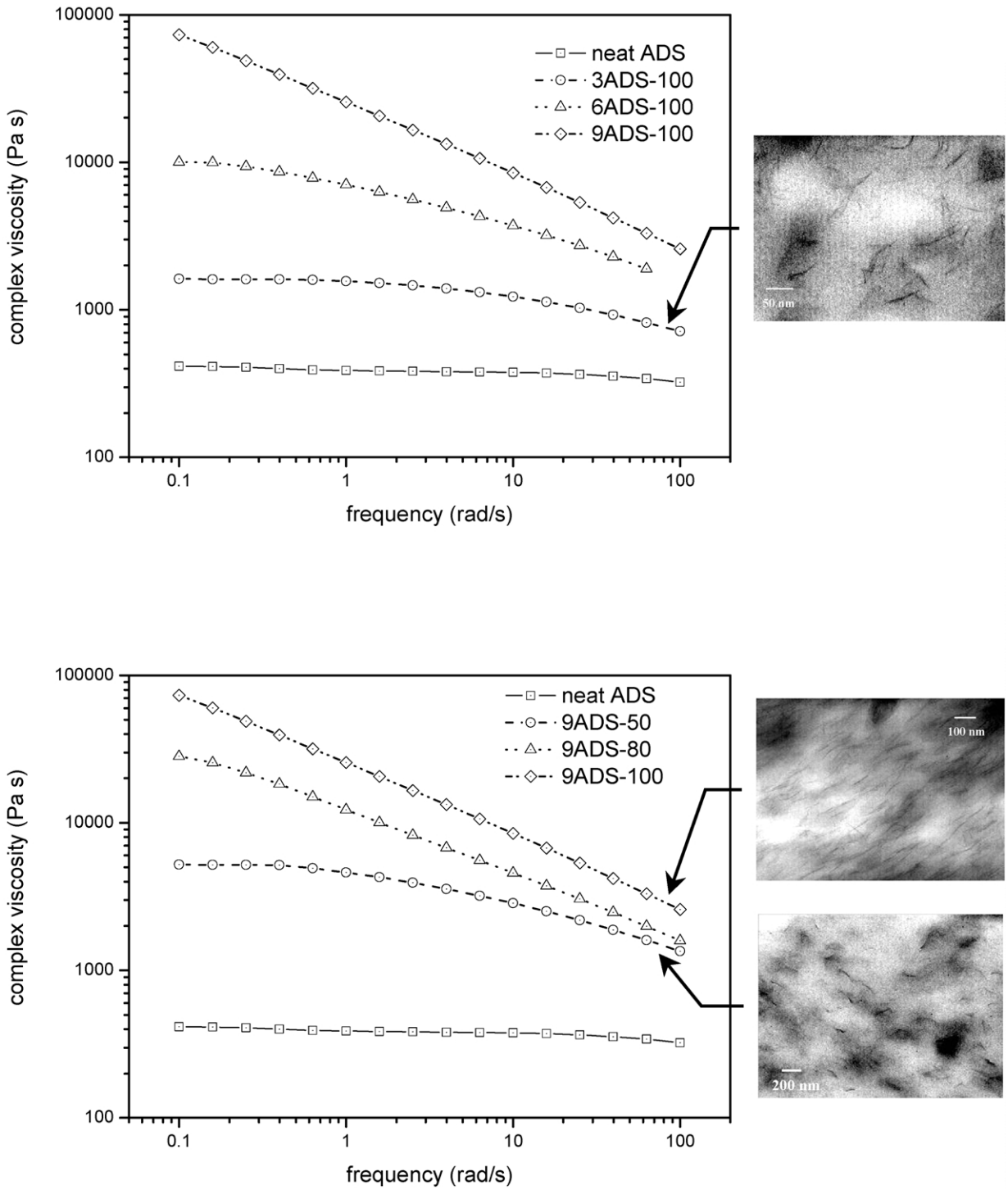

Fig. 3. (a, b) Complex viscosity curves ($T = 255$ °C, strain = 1%) and TEM micrographs for the ADS-based nanocomposites: effect of silicate loading (a) and extrusion rate (b).

thermoplastic composites: some studies [35] on dispersed flow of particulate-filled polymers, containing high percentage of fillers (glass spheres, barium sulfate or calcium carbonate powder), demonstrate that the dynamic viscosity increases with the filler concentration and, beyond a critical concentration, show a divergence at low frequencies indicating a structural change of the network formed by the particles. The exact concentration at which a continuous structural network forms depends on the nature of the filler, its size and the interactions between the filler and the suspending medium. The increments in complex viscosity observed in this study are comparable to those measured in composite systems having filler loadings in the range of 40–60 wt% [4,36]. The fine dispersion obtained in

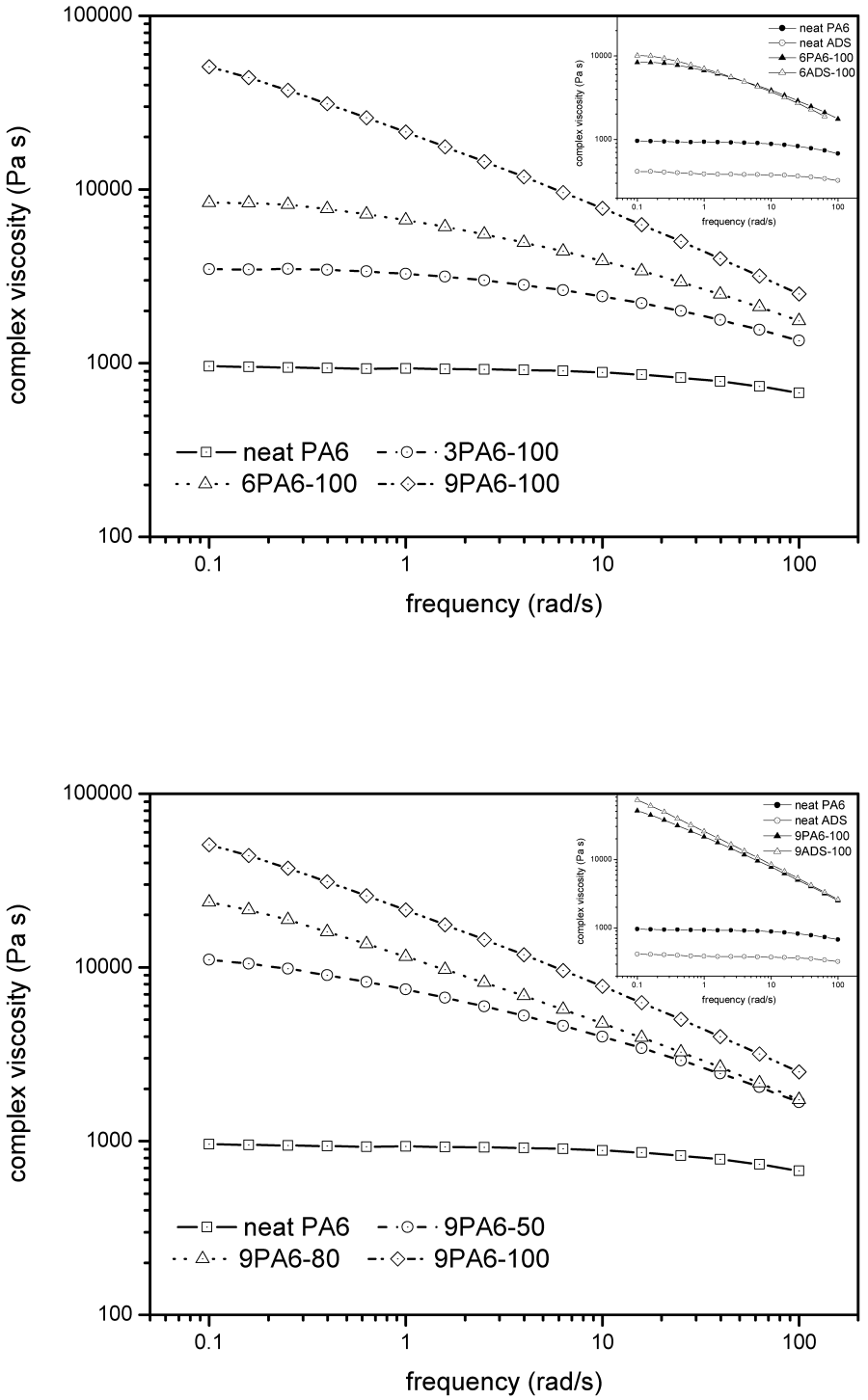

Fig. 4. (a, b) Complex viscosity curves ($T = 255$ °C, strain = 1%) for the PA6-based nanocomposites: effect of silicate loading (a) and extrusion rate (b). In the small inner graphs a comparison with the complex viscosity curves of the ADS-based hybrids is shown.

nanocomposites hybrids, together with the high aspect ratio and the shape of the silicate platelets, favors the formation of a structural network already at very low silicate content. Fig. 3(b) shows that the extrusion rate has the same effect of silicate content on the flow behavior: higher screw speeds realize a better dispersion of clay platelets, promoting the formation of a structural network expressed by pseudo-non-Newtonian shear thinning. Fig. 3(a) and (b) put also in evidence the link between the flow curve shape and the state of exfoliation and intercalation, inferred by TEM analysis and widely discussed in our previous work on preparation and characterization of ADS-based nanocomposites [29]. The micrographs of 3ADS-100, 9ADS-50 and 9ADS-100 are reported as example. It can be clearly observed that 3ADS-100 and 9ADS-50 samples, whose complex viscosity curves exhibit moderate deviations from pseudo-Newtonian trend, have a non-homogeneous silicate layers distribution in the polymer matrix, with a micron-scale morphology comprised of intercalated aggregates surrounded by a distribution of uncorrelated layers; instead, 9ADS-100 sample, whose complex viscosity curves is markedly shear thinning in the whole frequency range investigated, exhibits a more uniform dispersion of clay particles on micron-scale and a higher extent of silicate exfoliation on nanoscale with a macroscopic preferential orientation of the layers.

Similar trend can be observed in PA6-based nanocomposites (Fig. 4(a) and (b)), exhibiting a flow behavior comparable to that of ADS-based samples. Moreover, even if the ADS matrix has lower complex viscosity than PA6, the 6 and 9 wt% ADS-based nanocomposites show viscosity values comparable or slightly higher than the PA6-based ones produced at same extrusion rate (see comparisons between the complex viscosity curves of hybrids based on PA6 and ADS, shown in the small graphs inside Fig. 4(a) and (b)). Such results suggest that higher clay dispersion and exfoliation levels with stronger polymer–silicate interactions could be produced in ADS-based nanocomposites. The dispersion degree of a silicate in a polymer matrix, in fact, is the results of the stress transferred from the molten polymer to the clay platelets, which disrupt the clay particle in platelet tactoids, and of the polymer chain diffusion in the organoclay galleries, which leads to the 'peeling' of individual layers from clay tactoids [16]. At fixed processing conditions (temperature profile and shear rate), ADS matrix, that has lower viscosity, can transfer a reduced stress to the silicate but can diffuse faster between the layers with respect to PA6. Consequently, the level of intercalation–exfoliation reached in the two systems results from a balance of these counter-current effects.

The structural network formed in nanocomposites is emphasized by the behavior of the storage modulus (G'), extremely sensitive to morphological state. At this regard, the storage moduli of ADS-based nanocomposites extruded with different silicate content and screw speed are compared in Fig. 5(a) and (b). Analyzing the graphs it can be observed that G' monotonically rises at all the frequencies increasing both the silicate amount in the blend and the extrusion rate. Moreover, increasing the silicate content, the G' frequency-dependence at low ω decreases, suggesting that the polymer chains cannot be fully relaxed, as a consequence of the polymer–clay interactions.

The plots of storage (G') and loss (G'') moduli versus ω for ADS and PA6 based nanocomposites extruded at 100 rpm are reported in Figs. 6 and 7, respectively. The graphs show that both G' and G'' increase monotonically with the frequency for all samples, increasing the silicate content. Moreover, G' exhibits a stronger frequency dependence than G'' for the 3 wt% samples, as expected for melt polymers, whereas in the case of 6 and 9 wt% ones the frequency dependence of two moduli is almost equal. In particular, for the 9ADS-100 sample the G' and G'' curves are superimposed in all frequency range investigated. Such results indicate that, increasing the silicate amount in the hybrids, their viscoelastic response changes from a pseudo-liquid like behavior to a pseudo-solid like one. This change is more marked in percentage for nanocomposites based on

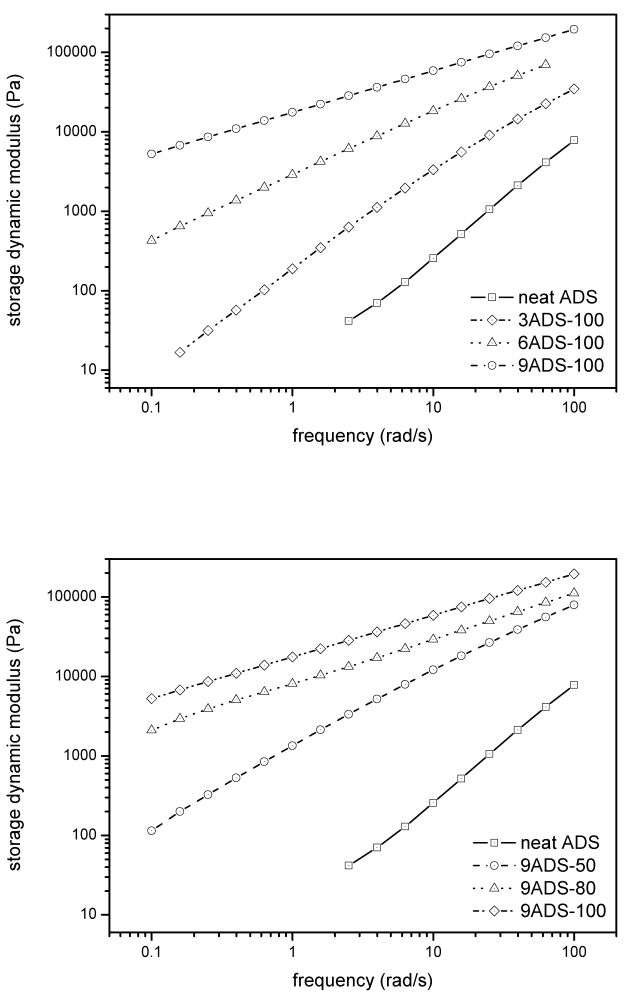

Fig. 5. (a, b) Storage modulus (G') vs. frequency ($T = 255$ °C, strain = 1%) for the ADS-based nanocomposites: effects of silicate loading (a) and extrusion rate (b).

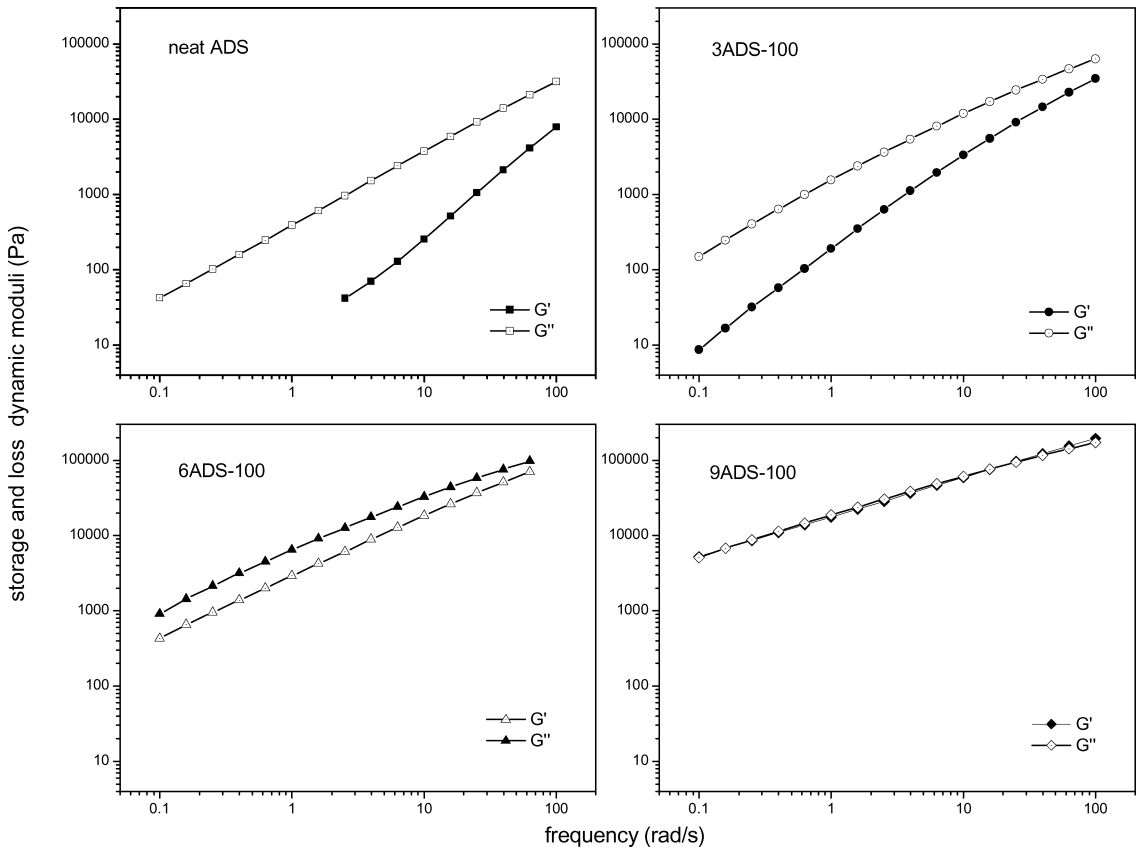

Fig. 6. Storage (G') and loss (G'') moduli vs. frequency ($T = 255$ °C, strain = 1%) for ADS-based nanocomposite systems, extruded at 100 rpm.

ADS copolyamide than for systems based on PA6 homopolymer.

The same outcome results also from linear stress relaxation tests performed on these hybrids. It is well known, in fact, that the dynamic oscillatory shear moduli G' and G'' are related to the linear stress relaxation via the relaxation spectrum $H(\tau)$ [37]:

$$G'(\omega) - G(t)|_{t=1/\omega} = \int [[(\omega^2\tau^2)/(1+\omega^2\tau^2)] - e^{(-1/\omega\tau)}]H \, d(\ln \tau)$$

Transient stress relaxation measurements, obtained at low strain in order to assure linear regime, are reported in Fig. 8 for ADS based nanocomposites. It can be observed that, for any fixed time after the imposition of strain, the modulus $G(t)$ increases with silicate loading, similarly to that observed in the dynamic viscoelastic measurements. Furthermore, while at short times the stress relaxation behavior is qualitatively similar for the hybrids and unfilled polymer, at long times the unfilled polymer relaxes like a liquid, while the hybrids with high silicate contents behave like a pseudo-solid material. Similar trend was observed also for PA6-based nanocomposites, but in this last case the differences are smaller (Fig. 9).

Both the dynamic oscillatory shear and the stress relaxation moduli indicate that the addition of the layered silicate to PA6 and ADS resins significantly modify the long-time relaxation of the hybrids increasing their relaxation times due to the formation of a three-dimensional superstructure. This phenomenon is particularly relevant for ADS hybrids with silicate loading higher than 6 wt%.

In order to measure the viscoelastic properties as a function of temperature, a dynamic mechanical analysis was performed. The DMA results for the dynamic storage modulus (E') were reported in Fig. 10, where the effect of clay percentage on the temperature dependence of E' for ADS-based nanocomposites is shown: the samples exhibit higher and higher storage modulus as increasing the silicate loading, resulting in a remarkable increase of stiffness, more evident at lower temperatures. The reinforcement effect becomes larger also with the extrusion rate, at fixed silicate amount [29]. Moreover, increasing the clay content a shift in the glass–rubber transition towards higher temperatures was also found: in particular, the T-position of the main peak in the E'' curve was shifted from about 60 °C, for the neat ADS, to about 70 °C, for all the hybrids [29]. The influence of clay on glass transition may be attributed to the confinement of polymer chains in silicate galleries that partially hinders the molecular motions. Although an increase in the T_g was also found by other researchers in many inorganic–polymeric nanocomposite systems [38], this is a not general finding. In fact, Giannelis et al. have shown that polymer chains in nanocomposites can exhibit

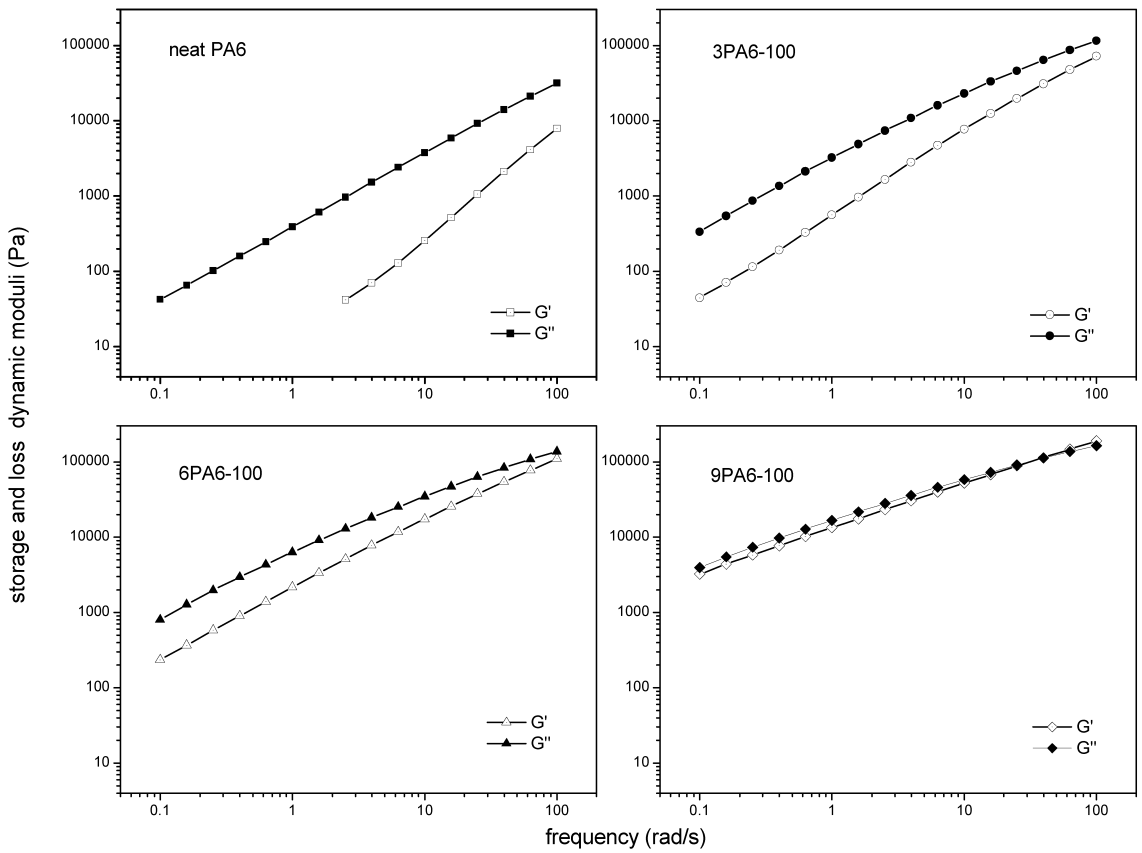

Fig. 7. Storage (G') and loss (G'') moduli vs. frequency ($T = 255$ °C, strain = 1%) for PA6-based nanocomposite systems, extruded at 100 rpm.

liquid-like mobility even below the bulk polymer T_g, explaining such unexpected behavior with the presence of polymeric low density areas having increased mobility at the organic–inorganic interface [10].

In view of possible technological applications of these nanocomposites, we have also analysed their viscoelastic response under the application of a steady shear flow field, that plays a critical role for the processability of polymer systems. At this regard, steady shear viscosity measurements were performed using a rotational rheometer. The results obtained on neat ADS matrix and 6ADS-100 nanocomposite are reported in Fig. 11, where also the complex viscosity curves are shown for comparison. The graph clearly evidences that the addition of even small quantities of clay to neat ADS significantly modifies the steady shear viscoelastic response of the copolyamide matrix in a similar way to that previously discussed for the dynamic frequency sweep tests. In fact, the steady shear flow curve of 6ADS-100 sample is approximately Newtonian only at low shear rate and deviates from this

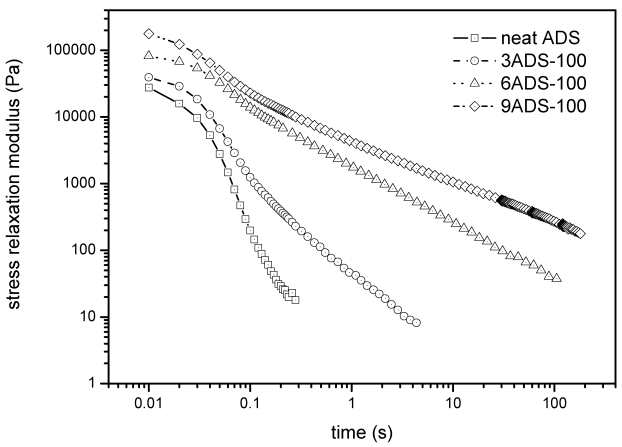

Fig. 8. Linear stress relaxation modulus $G(t)$ for ADS-based nanocomposites with different clay content, extruded at 100 rpm.

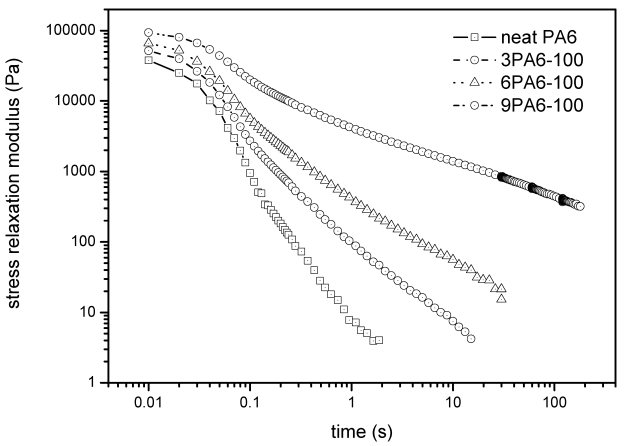

Fig. 9. Linear stress relaxation modulus $G(t)$ for PA6-based nanocomposites with different clay content, extruded at 100 rpm.

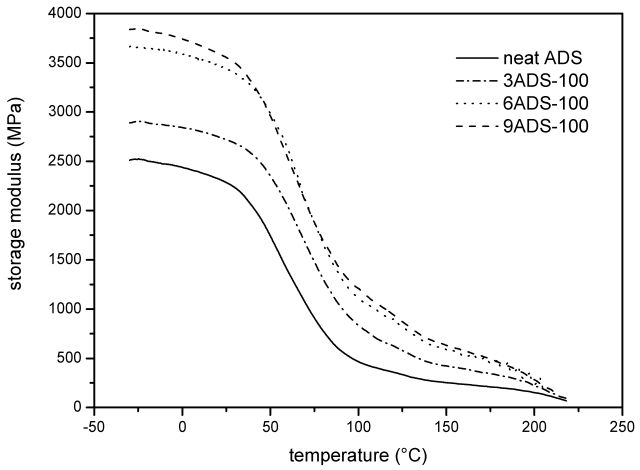

Fig. 10. Dynamic-mechanical storage modulus curves of ADS nanocomposite samples extruded at 100 rpm with different silicate loadings.

trend for $\dot{\gamma} \geq 0.3\ s^{-1}$. Moreover, it can be noted that the Cox-Merz rule [33,34], stating that:

$$\eta(\dot{\gamma}) = |\eta^*(\omega)|_{\dot{\gamma}=\omega} \quad [\omega] = \text{rad/s}, \ [\dot{\gamma}] = 1/\text{s},$$

is verified for the neat copolyamide and fails for the hybrid. The complex viscosity exceeds the steady shear viscosity, with the discrepancy being largest in the higher shear rate region, as expected. The effect increases with the clay loading (data not shown). These results, observed also for other filled and mesostructured polymer systems, suggest that the silicate layers may be oriented in the flow direction even in a rather low shear environment and give a further evidence that a domain structure with strong polymer–silicate interactions exists in the hybrids [4,31,37,39,40].

4. Conclusions

In this paper the rheological behavior of new copolyamide-based nanocomposites produced by melt compounding of the ADS copolymer, having a partially aromatic structure, with a commercial organo-modified montmorillonite, was investigated. Since viscoelastic measurements are highly sensitive to the nanoscale structure of materials, they were used as a powerful method to probe the developed morphology of nanocomposite materials. At this regard, rheological experiments (dynamic frequency sweep, steady rate sweep and stress relaxation tests) were performed and their results were related to TEM measurement observations. The study was performed on hybrids at three silicate loadings (3, 6 and 9 wt%), prepared by means of a laboratory-scale twin screw extruder, using different screw speeds (50, 80 and 100 rpm). Moreover, to highlight the effect of comonomer on the polymer–clay affinity and then on the morphology of the hybrids, all the experiments were replicated on nanocomposite samples produced at the same processing conditions using a polyamide 6 homopolymer as a matrix and the obtained results were compared.

The study put in evidence that the flow curve shape of the nanocomposites is associated to the exfoliation and intercalation level of the silicate platelets in the polymer matrix: hybrids, exhibiting complex viscosity curves with moderate deviations from pseudo-Newtonian trend, have a not very homogeneous clay layers distribution in the polymer matrix, with a micron-scale morphology comprised of intercalated aggregates surrounded by a distribution of uncorrelated layers; instead, samples, whose complex viscosity curves is markedly shear thinning, have a more uniform dispersion of clay particles on micron-scale and a higher extent of silicate exfoliation on nanoscale with a macroscopic preferential orientation of the layers. These hybrids show also a pseudo-solid-like flow behavior at long times, due to the occurrence of strong polymer–silicate interactions that slow the relaxation times of the polymer chains. The gradual transition from the pseudo-liquid-like relaxation to pseudo-solid-like flow behavior is realized in the hybrids extruded at rate higher then 80 rpm with clay amount higher than 6%. All these effects are more marked for nanocomposites based on the copolyamide matrix, suggesting that this resin may have a higher silicate affinity respect to polyamide 6 homopolymer.

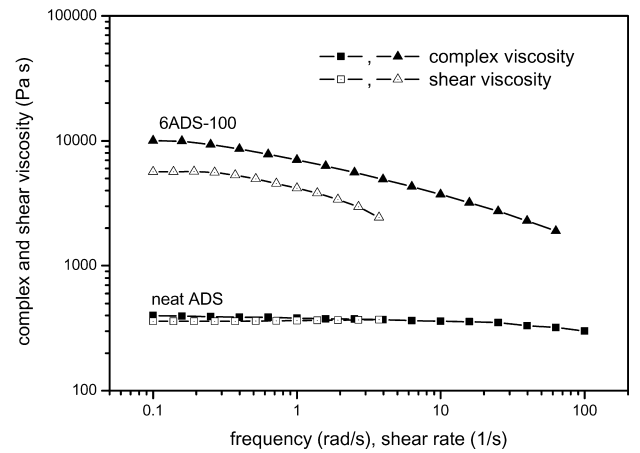

Fig. 11. Comparison between the dynamic and steady shear flow viscosity curves for the neat ADS and the 6ADS-100 nanocomposite.

Acknowledgements

This work was supported by PRIN Project 2001 (Title: Processability and film production of polymer–silicate nanocomposites by melt compounding). The authors acknowledge Dr Giovanna Maria Russo from University of Salerno (Italy), for working on this project.

References

[1] Osborn KR, Jenkins WA. Plastic films: technology and packaging applications. Lancaster: Technomic Publishing Company, Inc; 1992.

[2] Zilberman M, Siegman A, Narkis M. Polymer 1995;36:5065–7.
[3] Siciliano A, Severgnini D, Seves A, Pedrelli T, Vicini L. J Appl Polym Sci 1996;60:1757–64.
[4] Pinnavaia TJ, Beall GW, editors. Polymer-layered silicate nanocomposites. New York: Wiley; 2001.
[5] Alexandre M, Dubois P. Mater Sci Engng 2000;28:1–63.
[6] LeBaron PC, Wang Z, Pinnavaia TJ. Appl Clay Sci 1999;15:11–29.
[7] Holmes M. Plast Add Comp 2000;7/8:34–6.
[8] Messersmith PB, Giannelis EP. J Polym Sci, Part A: Polym Chem 1995;33:1047.
[9] Burnside SD, Giannelis EP. Chem Mater 1994;6:2216.
[10] Schmidt D, Shah D, Giannelis EP. Current opinion in solid state and materials science 2002;6:205–12.
[11] Shelley JS, Mather PT, DeVries KL. Polymer 2001;42:5849–58.
[12] Vaia RA, Jandt KD, Kramer EJ, Giannelis EP. Macromolecules 1995; 28:8080–5.
[13] Vaia RA, Jandt KD, Kramer EJ, Giannelis EP. Hem Mater 1996;8: 2628–35.
[14] Liu TX, Liu ZH, Ma KX, Shen L, Zeng KY, He CB. Compos Sci Technol 2003;63:331–7.
[15] Krishnamoorti R, Vaia RA, editors. Polymer nanocomposites. Synthesis, characterization and modeling. ACS Symposium Series No. 804, Washington, DC: American Chemical Society; 2002.
[16] Cho JW, Paul DR. Polymer 2001;42:1083–94.
[17] Fornes TD, Yoon PJ, Keskkula H, Paul DR. Polymer 2001;42: 9929–40.
[18] Dennis HR, Hunter DL, Chang D, Kim S, White JL, Cho JW, Paul DR. Polymer 2001;42:9513–22.
[19] Fujiwara S, Sakamoto T. Japanese Kokai Patent Application No. 109998; 1976 (assigned to Unichika K.K., Japan).
[20] Okada A, Fukushima Y, Kawasumi M, Inagaki S, Usuki A, Sugiyama S, Kurauch T, Kamigaito O. United States Patent No. 4739007; 1988 (assigned to Toyota Motor Co., Japan).
[21] Kawasumi M, Kohzaki M, Kojima Y, Okada A, Kamigaito O. United States Patent No. 4810734; 1989 (assigned to Toyota Motor Co., Japan).
[22] Usuki A, Mizutani T, Fukushima Y, Fujimoto M, Fukumori K, Kojima Y, Sato N, Kurauch T, Kamigaito O. United States Patent No. 4889885; 1989 (assigned to Toyota Motor Co., Japan).
[23] Yasue K, Tamura T, Katahira S, Watanabe M. Japanese Kokai Patent Application No. 248176; 1994.
[24] Maxfield M, Christiani BR, Murthhy SN, Tuller H. United States Patent No. 5385776; 1995.
[25] Christiani BR, Maxfield M. United States Patent No. 5747560; 1998.
[26] Davis RD, Gilman JW, VanderHart DL. Polym Deg Stab 2003;79: 111–21.
[27] Kubota H, Nowell JB. J Appl Polym Sci 1975;19:1521–38.
[28] Scarfato P, Di Maio L, Incarnato L, Acierno D, Mariano A. Packag Techn Sci 2002;15(1):9–16.
[29] Incarnato L, Scarfato P, Russo GM, Di Maio L, Iannelli P, Acierno D. Polymer 2003;44:4625–34.
[30] Krištofic M, Marcincin A, Ujhelyiová A. J Therm Anal Calorim 2000; 60:357–69.
[31] Krishnamoorti R, Yurekli K. Curr Opin Colloid Interface Sci 2001;6: 464–70.
[32] Pignon F, Magnin A, Piau JM. Phys Rev Lett 1997;79:4689–92.
[33] Dealy JM, Wissbrum KF. Melt rheology and its role in plastics processing. Dordrecht: Kluwer Academic Publishers; 1999.
[34] Ferry JD. Viscoelastic properties of polymers, 3rd ed. New York: Wiley; 1980.
[35] Liu L, Qi Z, Zhu X. J Appl Polym Sci 1999;71:1133–8.
[36] Han CD. Multiphase flow in polymer processing. New York: Academic Press; 1981.
[37] Krishnamoorti R, Vaia RA, Giannelis EP. Chem Mater 1996;8: 1728–34.
[38] Ash BJ, Schadler LS, Siegel RW. Mater Lett 2002;55:83–7.
[39] Medellin-Rodriguez FJ, Burger C, Hsiao BS, Chu B, Vaia R, Phillips S. Polymer 2001;42:9015–23.
[40] Ren J, Krishnamoorti R. Macromolecules 2003;36:4443–51.